IEEE Access
Multidisciplinary ⋮ Rapid Review ⋮ Open Access Journal

Received May 12, 2020, accepted June 7, 2020, date of publication June 11, 2020, date of current version July 1, 2020.

Digital Object Identifier 10.1109/ACCESS.2020.3001686

A Digital Twin for Operational Evaluation of Vertical Transportation Systems

MIKEL GONZÁLEZ[1,2], OSCAR SALGADO[1], JAN CROES[2,3], BERT PLUYMERS[2,3], AND WIM DESMET[2,3]

[1]Ikerlan Technology Research Centre, Basque Research and Technology Alliance (BRTA), 20500 Mondragón, Spain
[2]Department of Mechanical Engineering, KU Leuven, 3001 Leuven, Belgium
[3]DMMS Laboratory, Flanders Make, 3001 Leuven, Belgium

Corresponding author: Oscar Salgado (osalgado@ikerlan.es)

This work was supported in part by the European Commission for its support of the Marie-Sklodowska Curie Program through the ITN Advanced Training and Research in Energy Efficient Smart Structures (ANTARES) Project under Grant GA 606817, and in part by the KU Leuven Research Fund.

ABSTRACT The Digital Twin (DT) is a promising concept which aims at creating a virtual replica of an individual system, that can provide information otherwise not available. This paper presents a DT of a vertical transportation system, focusing on how to model this DT, and using it to evaluate the system condition and potential corrective solutions. Exploiting the advantages of object-oriented modeling, this DT has been built ensuring that it may be dynamically adapted to different monitoring scenarios. Moreover, its adaptability is tested showing that reduced models behave similarly. The resulting reduced models are used to estimate installation parameters in a bottom-up way, using the measurements of a scaled test bench. The estimated parameters are used to update a high-fidelity model and simulate the effect of corrective actions.

INDEX TERMS Digital twin, Kalman filter, state/parameter estimation, virtual sensing.

I. INTRODUCTION

Due to the latest advances in information and communication technologies, the advantages of modeling and simulation may now be used not only during design phases, but also during operational phases [1]. This opens the way to continuously simulate and update with measurements a virtual replica of the system. Such a replica may give insight into the system's behavior, for instance by (i) providing virtual sensors that extend available data [2], [3], (ii) generating synthetic data to feed machine learning algorithms [4], (iii) providing indicators of the system's condition [5], or (iv) simulating potential operational decisions to aid decision making. This concept is referred to as Digital Twin (DT). According to Glaessgen [6], the "DT is an integrated multi-physics simulation of a system, that uses the available physics-based models, sensors and fleet history to replicate the behavior of its real counterpart". Depending on the available resources and the required monitoring scenario, the DT's models may range from data-driven models to high-fidelity physics-based models. However, it is probably the physics-based models the ones which fully unleash the DT's potential [7], as physical insight is generally required to simulate situations that have not yet occurred.

One of the DT's main challenges is to ensure its models' accuracy regardless of the system's changes [8], such as component degradation or changes due to maintenance actions. The DT's models need to be updated as often as possible to reliably reflect the system's behavior. Parameter [9]–[11] and state estimation strategies [12]–[14] are attractive solutions to keep the DT updated. However, such strategies are not necessarily compatible with the high-fidelity models often required to address all the physics of interest. Generally, model parameters need to be estimated in a bottom-up way, i.e. starting at component level, which likely requires a dedicated model of the component. Moreover, in systems with a limited number of sensors, high-fidelity models with several states will likely result in non-observable systems, hindering the application of estimation algorithms [15]. Thus, the DT's models should be developed in a way that facilitates their adaptation to different scenarios, such as high-fidelity simulation, parameter estimation or state estimation, ensuring the suitable fidelity for each case. To this end, some authors have highlighted the necessity of building the DT as an adaptable[1] reference model, making it as generic as possible [16].

A DT is thus an attractive solution to systematically supply information which otherwise remains hidden, such

The associate editor coordinating the review of this manuscript and approving it for publication was Yue Zhang.

[1]In this study, model adaptability is referred to the model's ability to change its abstraction level, adapting to different monitoring scenarios.

as non-measured variables [3], system degradation and unknown operational conditions [6], or trends in the quality a manufacturing process. This information may thus provide a significant added value in the management of different assets. For instance, aiding in the rapid qualification of manufactured parts [17], providing maintenance suggestions [18], or suggesting manufacturing plant reconfiguration to ramp-up or to improve manufacturing quality [19]. Although the DT is a promising concept for several fields, there are many conceptual ideas, but few practical application examples. Moreover, a significant part of the DT literature seems to forget a key aspect of the DT, which is the connection with real measurements to make it a reliable replica [20]. In addition, there are still no defined rules on how to build such DT in a generic and adaptable way [21].

Vertical Transportation Systems (VTSs) are complex systems which could benefit from DTs. In particular, the evaluation of VTS's guiding system could be improved with the information provided by the DT. Together with faults in the electric machine, the faults in the guiding system have the highest effect on energy efficiency and comfort [22]. Such faults are mainly due to guide misalignment and bumps in the guide joints [5]. Most of the guiding system monitoring strategies of the literature rely on complex devices to measure the guide's deviation [23]–[25].

Other techniques rely on data-driven techniques, for instance by processing the cabin acceleration signal [26] or the machine currents [27]. Likely, such data-driven techniques result in cost efficient methods, but the performance of extrapolating a data-driven strategy to other installations or operational conditions is not always guaranteed [28]. For instance, as discussed by Skog [26], elevator speed must be considered when using vibration for condition monitoring. Similarly, when using machine currents for guide system evaluation, the effect of cabin and counterweight load and acceleration profile should be considered. Thus, the thresholds set-up in the initial training phase will probably depend on operational conditions and characteristics of each individual installation. In this context, a DT based on first-principles models could aid in the assessment of VTSs. By combining this DT with available sensors, it may provide valuable information, for instance, by (i) estimating condition-sensitive parameters, (ii) estimating virtual sensors, or (iii) simulating potential operational actions.

The aims and novelty of this study are (i) to create an adaptable model of a VTS that cost efficiently adapts to the required monitoring scenario, (ii) to use the reduced models to estimate the guiding system's profile in a bottom-up way, (iii) to use the estimated profile as an indicator of the guide's condition, and (iv) to use the estimated feature to update the VTS's DT, and simulate potential operational actions.

II. DIGITAL TWIN FOR SYSTEM EVALUATION

As described earlier, a DT comprises a set of models representing specific aspects of the system. These models include data-driven models, CAD models and physics-based models. This paper deals exclusively with a DT made of physics-based models, for which the following requirements have been identified:

- **Model reliability:** the DT shall not be a generic representation of a system, but rather a direct one-to-one replica of an individual asset. Model reliability is an essential aspect in the exploitation of the DT concept, and probably the primary factor differentiating traditional simulations and a DT. Among others, ensuring model reliability involves (i) using the same input and operational conditions as the real system, and (ii) updating the models as often as possible with the sensors available. Thus, the DT should have means to combine the models with the available measurements [20].
- **Model adaptability:** a holistic model aiming at representing every aspect of the real system may seem the most straightforward option. However, depending on the scope of the DT, it may not be feasible. Most likely, a number of models are required to represent different aspects of the system and to address different scenarios, such as bottom-up parameter estimation, state estimation or high-fidelity simulation. To ensure modeling cost-efficiency, model adaptability and reusability should be fostered.
- **Model distribution:** models shall be accessible by different monitoring algorithms. Thus, models and estimation/simulation tools should be made as generic as possible, ensuring compatibility regardless of their origin. Ensuring the compatibility of different models and tools also fosters the envision of a DT made of several models, where (i) the expertise of specialized software in certain domains can be exploited, and (ii) models generated by different suppliers/partners can be used together regardless of the tool of origin.
- **Accessibility:** the use of simulation models is still a task for experts. The outcome of a DT for monitoring applications should be made as understandable and accessible as possible by non-experts.

Figure 1 depicts the framework proposed to address these requirements. This framework consists of the following components:

1) **Digital Twin:** this is a virtual replica of the system, which runs in parallel and with the same operational conditions as the real system. It is composed of several models representing different aspects of the system, such as (i) high-fidelity models simulated in open-loop to understand and predict the system's behavior, and (ii) reduced estimation models blended with the available measurements to obtain unknown parameters. The set of estimation models, and the tools used to combine them with measurements, are crucial to fulfill the requirement of ''model reliability''. Section IV-B provides a practical example where the guiding system's profile is estimated through joint state-parameter estimation.

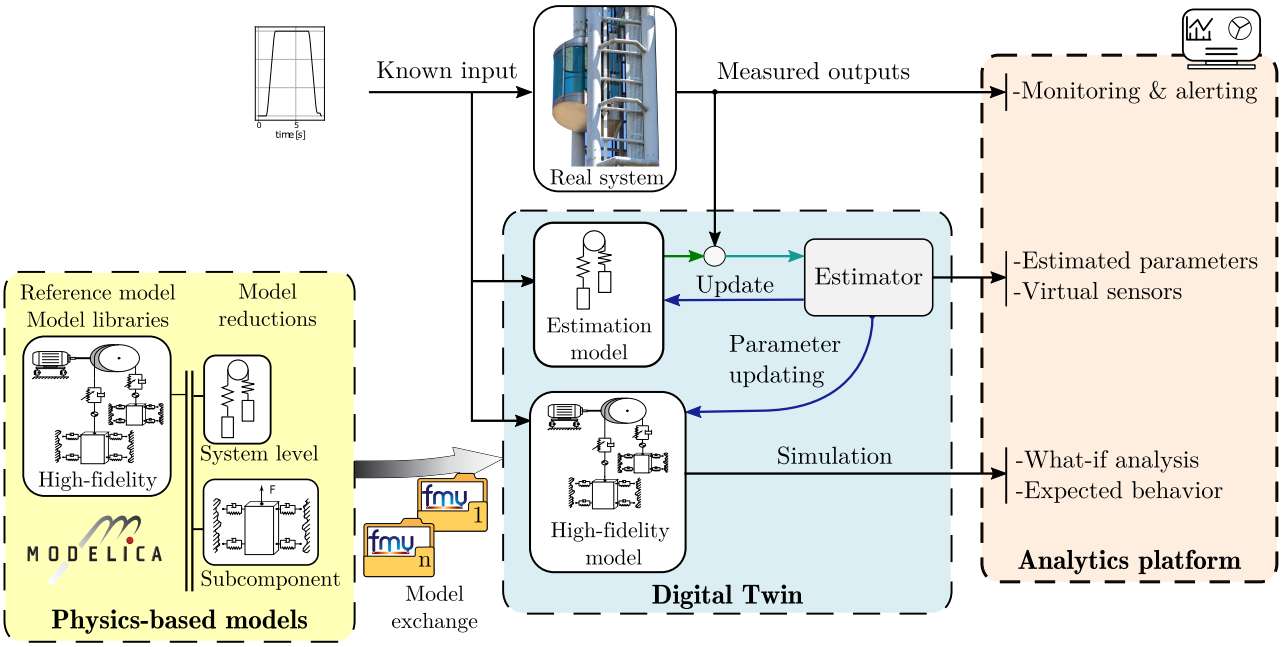

FIGURE 1. Elements of the presented framework.

2) **Reference model/model library:** this element refers to the means to obtain the physics-based models that will be used by the DT, addressing the requirements of model adaptability and distribution. It may consist of a reference model with capacity to adapt its fidelity level automatically, a library of model components, or a set of predefined models. The goal of this component is to provide models with the suitable fidelity for a specific problem [29]. Object-oriented modeling tools are a potential solution for lumped parameter models. There, model adaptability may be achieved by making certain Degrees of Freedom (DoF) depend on user parameters. More specifically, this work uses the acausal modeling tool Modelica [30]. Section III describes how an adaptable model can be generated by constraining certain states with user-dependent Boolean parameters. These models need to be distributed in a way that facilitates their use by the DT's simulation and estimation tools. In this work, the Functional Mock-up Interface (FMI)[2] for model exchange is used to convert models into generic models that can be used with general purpose programming languages, ensuring the compatibility regardless of the modeling tool. Furthermore, models exchanged through the FMI are described as ODEs, as preferred by most estimation algorithms. Thus, the acausal models are converted according to the FMI, and supplied to the DT as Functional Mock-up Units (FMU).
3) **Analytics platform:** this is the platform which leverages on the information provided by the DT to indicate the condition of the system, and to provide operational suggestions. The development of such a platform is out of the scope of this paper. Instead, Sections IV-C and IV-D show how simulated time series may be converted into performance indicators, easier to transfer and to understand than time series.

[2]https://fmi-standard.org/, last accessed 07/02/2020

III. REFERENCE MODEL OF A VERTICAL TRANSPORTATION SYSTEM

This section presents a reference model of VTSs, this is, a model which can adapt its fidelity to different scenarios. This reference model has the same main components as the real installation. Next, these components and their respective models are described. This model uses Modelica's Multi-Body library [31]. In this library, the "Frame" component is used to connect different components, ensuring force and torque balance, and setting the position and orientation of each of the connected components to be the same.

- **Cabin model:** the cabin is the component carrying the payload, which is balanced with a counterweight to improve energy efficiency. The same model is used for both cabin and counterweight, which are modeled using a rigid-body model, i.e. three translations and three rotations. The dynamics of this body are represented by the Newton-Euler equations

$$\sum_i \mathbf{F_i^0} = m \cdot (\mathbf{a_0} + \dot{\omega_0} \times \mathbf{r_{cm}^0} + \omega_0 \times (\omega_0 \times \mathbf{r_{cm}^0})) \quad (1)$$

$$\sum_i \mathbf{M_i^0} = \mathbf{I} \cdot \dot{\omega_0} + \omega_0 \times (\mathbf{I}.\omega_0) + \mathbf{r_{cm}^0} \times \mathbf{F_i^0} \quad (2)$$

where $\mathbf{F_i^0}$ and $\mathbf{M_i^0}$ are the forces and moments applied at the origin of the coordinate system $\mathbf{0}$ located at the cabin's floor, $\mathbf{a_0}$ is the body's acceleration, ω_0 is the body's angular velocity, and $\mathbf{r_{cm}^0}$ is the position of the car's center of gravity. The cabin's translations and

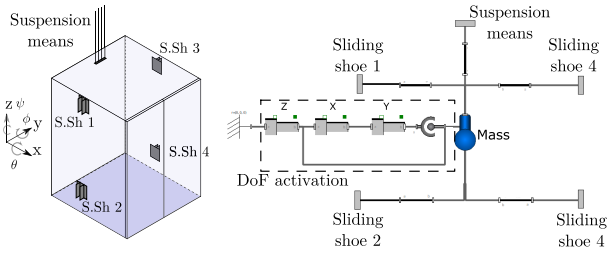

FIGURE 2. Cabin model with DoF selection built in Modelica.

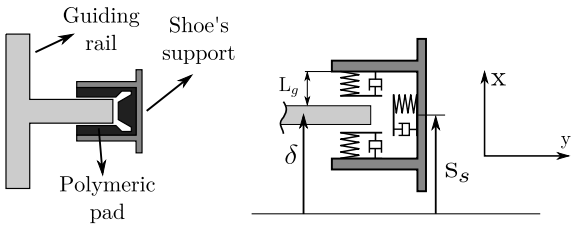

FIGURE 3. Idealization of guide-cabin contact.

rotations have been included to assess the effect of defects in the guiding system. However, it may often be better to neglect these DoF and account only for the cabin's vertical translation [32], [33]. Therefore, this sub-model has been developed in such a way that the end-user may define whether rotations and horizontal translations are allowed. Figure 2 illustrates[3] an alternative to develop such model. The elements within the "DoF activation" square depend on a Boolean user-parameter which if activated, constraints the X, Y and rotational DoF by directly connecting the vertical translation (z) DoF with the body. Additionally, it can be seen that this model has five connector frames. Four of them are devoted to the connection with the guiding system, and the fifth one connects the cabin with the suspension means.

- **Guiding system:** it consists of two steel rails which bound the cabin's horizontal movement. Generally, the cabin has four sliding shoes, which grab the guiding rail's web contacting it in three flanges. This contact is modeled with an event driven spring-damper system [34], which is only active when it contacts the guiding rail. Deviations in the guiding rail's riding path, such as out-of-angle and out-of-plane misalignment, lead to increased contact and friction forces. It is therefore of special interest to take such defects into account in the guiding rail's model. To do that, the guiding rail's profile is introduced in the contact model as an external input which adds to the initial spring length of the contact spring element, δ_x and δ_y for the x and y directions respectively. This leads to a contact force as

$$F_N = \begin{cases} 0 & s_s - \delta > L_g \\ K(s_s - \delta - L_g) & s_s - \delta \leq L_g \end{cases} \tag{3}$$

where F is the contact force, K is the contact stiffness, s_s is the sliding shoe's position, δ is the guide's position, and L_g is the sliding shoe's clearance. Figure 3 shows schematically the idealization of this contact.
Since the alignment of the guiding system changes along the installation's height, the contact forces with the guide will also change. Therefore, friction forces will change along the trip, mainly due to the change of the normal force exerted between the guide and the sliding shoes. This change is assumed to be the dominant cause of friction change. In addition, since the elevator is mostly traveling at a constant speed, only *sliding regime* friction is considered. Therefore, a Coulomb friction model with a constant friction coefficient is used as

$$F_f = \mu F_N \tag{4}$$

where F_f is the friction force, μ is the friction coefficient, and F_N is the normal contact force. If the cabin's transnational and rotational DoF are neglected, this model is not accounted for anymore. Instead, the friction forces are considered as an absolute resultant force acting on the center of the cabin, and are introduced as an external input.

- **Suspension means:** the suspension cable is the element which couples the cabin's vertical movement with the pulley and the electric machine. As described in [33], the cable may be modeled as two independent springs, one for the cabin's side and one for the counterweight. In addition, the cable's mass is also accounted for, as it also increases the system's load. Due to the change in cable length as the cabin travels, these cables are modeled as springs with a varying stiffness and mass, defined as [33]

$$L_c = L_0^c + R_p\varphi \tag{5}$$
$$L_{cw} = L_0^{cw} - R_p\varphi \tag{6}$$
$$K_c = \frac{\mathrm{EA}\cdot \mathrm{n}}{L_c} \tag{7}$$
$$K_{cw} = \frac{\mathrm{EA}\cdot \mathrm{n}}{L_{cw}} \tag{8}$$
$$m_c = \lambda_m \cdot L_c \tag{9}$$
$$m_{cw} = \lambda_m \cdot L_{cw} \tag{10}$$

where L_c and L_{cw} are the cable's length at cabin and counterweight sides, R_p is the pulley's radius, φ is the machine's angular position, K_c and K_{cw} are the cable stiffness, n is the number of cables, EA is the cable's longitudinal stiffness, m_c and m_{cw} are the cable's masses, and λ_m is the cable's longitudinal density.

- **Driving pulley:** this is the system which connects the cable and the electric machine. In this model, slip is neglected, and each side of the cable is assumed independent. The tension difference between the cabin and counterweight sides is assumed to be compensated by friction in the pulley. Consequently, the torque

[3]This figure is not a one-to-one capture of the model, it has been modified to facilitate its interpretation

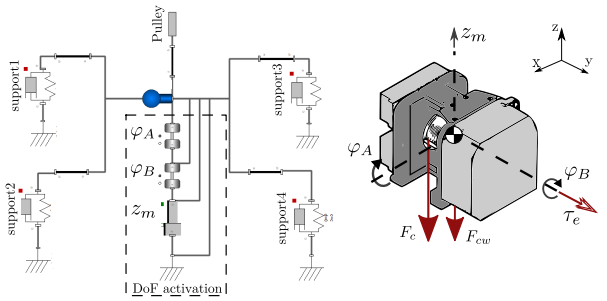

FIGURE 4. Model of the electric machine and its support built in Modelica.

balance in the pulley is

$$J_p\alpha = R_p(F_c - F_{cw}) + \tau_e + \tau_L \tag{11}$$

where J_p is the pulley's inertia, α is the pulley's angular acceleration, F_c is the cabin side's tension, F_{cw} is the counterweight side's tension, τ_e is the electric machine's torque, and τ_L is the friction loss torque. This component adds two states to the system, the pulley's angular position, φ, and angular velocity, ω.

- **Machine support:** the machine's vibration is also accounted for, as it may be an additional source of discomfort to be studied. The machine is generally supported on top of the guides, isolated with a rubber-like material. In the current model, the support is idealized, discretizing the support's position in four points. Figure 4 illustrates[3] a potential solution. As with the cabin, additional connections have been included to allow an efficient adaptability. Namely, through a user-defined parameter, the machine's inclination DoF may be neglected, accounting only for its vertical vibration. Similarly, all its DoF can be neglected, by fixing the machine's mass to the ground. Consequently, this element adds up to 3 DoF: one vertical translation, z_m, and two inclinations, φ_A, and φ_B.
- **Permanent Magnet Synchronous Machine (PMSM):** this is the type of gearless electric machine commonly used to move the system. The dynamics of the PMSM are represented in the direct-quadrature (d-q) reference frame as described in [35]. This reference system moves together with the machine's magnetic flux, leading to the following constitutive equations

$$V_q = Ri_q + L_q\dot{i}_q + p\omega(L_d i_d + \lambda) \tag{12}$$
$$V_d = Ri_d + L_d\dot{i}_d - p\omega(L_q i_q) \tag{13}$$
$$\tau_e = K_T i_q \tag{14}$$

where V_q and V_d is the quadrature and direct voltages, i_q and i_d are the quadrature and direct currents, ω is the machine's angular velocity, L_q and L_d are the inductances, R is the stator resistance, λ is the magnetic flux linkage, τ_e is the machine generated torque, and K_T is the machine's torque constant. This model leads to two states: i_d and i_q, which are the currents in the direct and quadrature axis respectively.

- **Control:** elevator PMSMs are commonly driven by a current-regulated inverter drive. Making use of the previously mentioned d-q reference frame, a Field-Oriented Control commands a zero d-axis current $i_{dref} = 0$, and the q-axis current is set to fulfill the required torque [35]. A common current control uses three PI loops: a q-axis current loop, a d-axis current loop, and a reference speed loop, which are governed by [33]

$$i_q^* = K_T\left(K_{p\omega}(\omega_{ref} - \omega) + \int_0^t \frac{K_{p\omega}}{T_{i\omega}}(\omega_{ref} - \omega)dt\right) \tag{15}$$

$$V_q = K_{pq}(i_{qref} - i_q) + \int_0^t \frac{K_{pq}}{T_{iq}}(i_{qref} - i_q)dt \tag{16}$$

$$V_d = K_{pd}(i_{dref} - i_d) + \int_0^t \frac{K_{pd}}{T_{id}}(i_{dref} - i_d)dt \tag{17}$$

where K_p is the loop proportional gain, and T_i is the integration time. In this model the inverter is omitted, and the computed voltage is introduced as an input in the previously described PMSM model. To facilitate its state-space description, an auxiliary state variable is introduced, $\dot{x} = u/T_i$, being u the input to the loop. Thus, the control loops are modeled as follows

$$y = K_p(u + x) \tag{18}$$

In total, this reference model has 37 states, but it may be scaled down by constraining certain states, or by obtaining standalone models from its components. Table 1 summarizes the reference model's states and compares the reference model with two reduced models derived from it: (i) a component level model, which represents exclusively the cabin and which uses as external input the tension in the cable, and (ii) a reduced system level model, where the lateral and rotational DoFs of cabin and counterweight are neglected. In addition, to better compare these model, this table summarizes for each model (i) the required external input, (ii) the model's goal, (iii) the generation method, (iv) the median computational time of 10 simulations of circa 6 s, and (v) a reference to an application case. The reference model provides a tool to assess the effect of guide defects on the overall performance of the installation, while the reduced models may be combined with estimation algorithms as suggested in [5], [33]. As previously described, this model reduction does not refer to a classical model order reduction consisting on a matrix space reduction. Rather, it consists of changing the model's equations, leveraging on the properties of object-oriented modeling. The choice of the model reduction scheme depends on the model at hand. In the current case, as the models are developed using acausal modeling tools, where the modeler has few control over the model structure, the described scheme of constraining certain DoFs was deemed the best option. With regards to computational time, the reduced models offer a significant time reduction at the cost of providing less information. These models are meant for estimation purposes, not as alternatives to improve simulation efficiency. This information is provided to highlight model differences.

TABLE 1. Comparison of reference and reduced models.

State description				Models		
Component	**Descripion**	**DoF**	**Units**	**Reference model**	**1D Model**	**Cabin Model**
Cabin	Vertical translation	z	[m]	●	●	●
	Lateral translation	x, y	[m]	●	○	●
	Rotations	θ, ϕ, ψ	[rad]	●	○	●
Counterweight	Vertical translation	z	[m]	●	●	○
	Lateral translation	x, y	[m]	●	○	○
	Rotations	θ, ϕ, ψ	[rad]	●	○	○
Pulley axis	Rotation	φ_p	[rad]	●	●	○
Machine support	Vertical translation	z_m	[m]	●	●	○
	Inclination	φ_A, φ_B	[rad]	●	●	○
PMSM	Currents	i_d, i_q	[A]	●	●	○
Controller	Aux. states (currents)	x_d, x_q	[A]	●	●	○
	Aux. states (speed)	x_ω	[rad/s]	●	●	○
	Model input			Reference speed, ω_{ref} [rad/s]	Ref. speed, ω_{ref} [rad/s], Friction forces, F_f [N]	Cable tension, F_c [N]
	Number of states			37	17	12
	Goal			Open-loop simulation	Virtual sensing	Estimation
	Model generation			Full model	Constraint DoF	Sub-component
	Computational time (median $\pm$ 2σ)			87.1 $\pm$ 16.5 s	11.5 $\pm$ 0.8 s	9.1 $\pm$ 0.8 s
	Application case			Sections III-A, IV-D	Section III-A, [3, 5]	Section IV-B

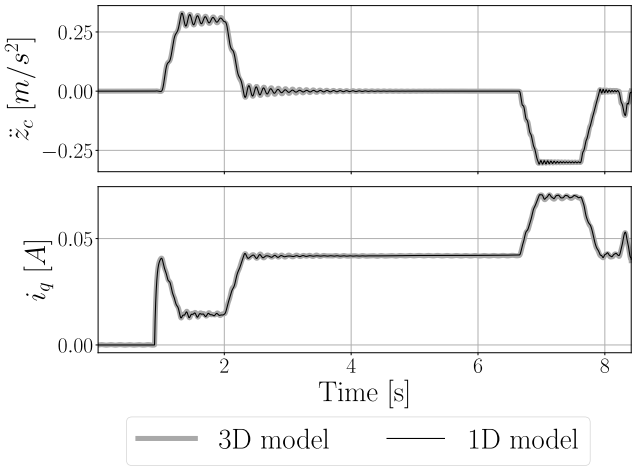

FIGURE 5. Comparison of the 1D and 3D elevator models.

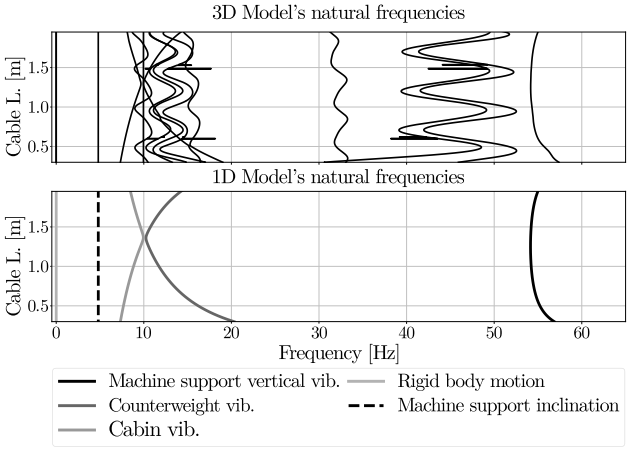

FIGURE 6. Linearized natural frequencies of the elevator models.

No assumption is made on the maximum computational cost acceptable for practical applications. Moreover, flexibility on model distribution was prioritized over model efficiency. Thus, the computational efficiency of these models could be highly improved.

A. MODEL REDUCTION

An important aspect when scaling down the model is to ensure that the reference and the reduced models have the same behavior in the shared physics. The neglected physics will not affect the scaled model, but the remaining DoF should have the same behavior. In this section, this is tested for the case where the cabin's lateral vibration and rotations are constrained, and the machine's support's movement has been reduced to a vertical vibration and out-of-axis inclination, leading to a 1D model with 17 states (Model 1D in Table 1).

Figure 5 compares the simulation of the 1D model and the reference model (3D model) for an ideal case, i.e. perfectly aligned guide. The friction forces computed in the 3D model are used as input in the 1D model. As can be seen, both models have roughly the same prediction. Slight negligible differences are possibly produced by the coupling between the cabin's vertical and rotational movement, which is not accounted for in the 1D model.

In addition to the time-domain simulation, the system's frequency response should also be the same for the shared dynamics. Figure 6 compares the linearized natural frequencies of the 3D and 1D models. These natural frequencies have been computed as

$$f = \frac{|\lambda|}{2\pi} \tag{19}$$

where λ are the eigenvalues corresponding to second order systems of the process matrix linearized at each time step. These natural frequencies are plotted against the cable's length, as this is the main cause for their change. As can be seen, both models have the same natural frequencies for the

modes corresponding to the vertical dynamics, whose origin has been labeled for the 1D model. For the 3D model, also several natural frequencies related to the cabin's rotation and lateral translation appear. However, due to the large number of DoF is not straightforward to identify their origin.

IV. APPLICATION CASE: GUIDE ALIGNMENT EVALUATION AND SOLUTION ANALYSES

As described earlier, the alignment of VTSs' guiding system is considered the dominant cause behind friction losses, and an important source of vibration and discomfort. Therefore, the goal here is to (i) estimate the guide's alignment, and (ii) use it to simulate the effect of guide reconfiguration on the installation's comfort and energy efficiency. We propose estimating the guide alignment as a model parameter which varies[4] along the guide's position. This parameter needs to be estimated in a bottom-up approach, estimating at component level so that other components do not affect the estimation [36], and the guide's effect is properly isolated from other sources of energy losses or discomfort. Therefore, a model representing only the cabin and the guiding system is extracted from the reference model and used in the estimation. The reference model itself is also used to simulate the potential effect of acting on the guiding system.

Particularly, this analysis is carried out in the VTS test bench presented in [37]. On top of the components described in Section III, the test bench has a 1:16 planetary gearbox to allow using a real electric machine and controller in a reduced height. This gearbox introduces unrealistic friction losses which are not present in a real installation. These losses are computed using a torque sensor and used as input in the model. The rest of the section is organized as follows. Firstly, the model identification strategy is described. Secondly, a model of the cabin and guiding system is used to isolate this subsystem and update the reference model in a bottom-up way. Next, with the updated reference model, different maintenance alternatives are simulated.

A. PARAMETER ESTIMATION STRATEGY

The selection of a parameter estimation strategy highly depends on the model and the nature of the parameters. In this case, the features of interest will be estimated using state estimators augmented with the unknown parameters/inputs [38]. In [39] joint state/parameter estimation was used together with an expectation maximization (EM) algorithm, showing that the optimal value is the mean value of the estimated parameter. Thus, when estimating a constant parameter, EM, least-squares, or heuristic optimization methods could be a more efficient option. However, in the current case the goal is to analyze parameter changes as a function of the guide's height. Thus, the estimated features will not be a single value, but rather an array function of the geometry. In addition, the evolution of the system's dynamic states has to be accounted for. Therefore, joint state/parameter estimation is deemed the better solution: state estimation accounts for the cabin's dynamics, while the augmented state provides the guide's profile.

In this work, an Extended Kalman Filter (EKF) is used. The EKF is the most widely used non-linear extension of the Kalman Filter [40]. The EKF assumes that the system behaves as a state space model disturbed by zero-mean white noise as

$$\begin{aligned}\dot{\mathbf{x}} &= \mathbf{f}(\mathbf{x}, \mathbf{u}, t) + \mathbf{w} \\ \mathbf{y} &= \mathbf{h}(\mathbf{x}, \mathbf{u}, t) + \mathbf{v}\end{aligned} \tag{20}$$

where $\mathbf{x}$ is the state vector, $\mathbf{y}$ is the system output, t is the time, $\mathbf{u}$ is the system input, and $\mathbf{w}$ and $\mathbf{v}$ are the process and measurement noise respectively. These noise terms are considered zero-mean random variables with covariance $\mathbf{Q}$ and $\mathbf{R}$ respectively. Similarly, the states are assumed to be Gaussian variables with a covariance $\mathbf{P}$, i.e. $\widehat{\mathbf{x}} = \mathbf{N}(\widehat{\mathbf{x}}, \mathbf{P})$. Given this model, and starting with an initial guess of the state vector and its covariance, i.e. $\hat{\mathbf{x}}_0^+$ and $\mathbf{P}_0^+$, the filter estimates the most probable value of the states [40].This is done in two steps, prediction and update. In the prediction step, an a-priori estimation of the states is obtained as

$$\hat{\mathbf{x}}_{k+1}^- = \mathbf{f}_k(\hat{\mathbf{x}}_k^+, u_k) \tag{21}$$

$$\hat{\mathbf{y}}_{k+1} = \mathbf{h}_{k+1}(\hat{\mathbf{x}}_{k+1}^-, u_k) \tag{22}$$

where $\hat{\mathbf{x}}_{k+1}^-$ is the a-priori state estimation, $\mathbf{f}_k$ and $\mathbf{h}_k$ are the discrete system functions, and $\hat{\mathbf{y}}_{k+1}$ is the predicted output. At each time step, the states covariance matrix is propagated using the linearized system matrix as

$$\mathbf{F}_k = e^{\frac{\partial \mathbf{f}_k}{\partial \mathbf{x}_k}\delta t} \tag{23}$$

$$\mathbf{H}_{k+1} = \frac{\partial \mathbf{h}_{k+1}}{\partial \mathbf{x}_{k+1}} \tag{24}$$

$$\mathbf{P}_{k+1}^- = \mathbf{F}_k \mathbf{P}_k^+ \mathbf{F}_k^T + \mathbf{Q}_k \tag{25}$$

where δt is the time step, $\mathbf{F}_k$ is the linearized discrete system matrix, $\mathbf{H}_{k+1}$ is the linearized output matrix, and $\mathbf{Q}_k$ is the process noise covariance. Next, this a-priori estimation of the states is updated using the available measurements. First, the residuals, i.e. the difference between the predicted and measured outputs, and their covariance are computed as

$$\mathbf{r}_{k+1} = \hat{\mathbf{y}}_{k+1} - \mathbf{y}_{k+1} \tag{26}$$

$$\mathbf{S}_{k+1} = \mathbf{H}_{k+1} \mathbf{P}_{k+1}^- \mathbf{H}_{k+1}^T + \mathbf{R}_k \tag{27}$$

where $\mathbf{r}$ is the residual, and $\mathbf{S}$ is its covariance. Finally, the a-posteriori state estimation and covariance estimation are computed as

$$\mathbf{K}_{k+1} = \mathbf{P}_{k+1}^- \mathbf{H}_{k+1}^T \mathbf{S}_{k+1}^{-1} \tag{28}$$

$$\hat{\mathbf{x}}_{k+1}^+ = \hat{\mathbf{x}}_{k+1}^- + \mathbf{K}_{k+1} \mathbf{r}_{k+1} \tag{29}$$

$$\mathbf{P}_{k+1}^+ = (\mathbf{I} - \mathbf{K}_{k+1} \mathbf{H}_k) \mathbf{P}_{k+1}^- \tag{30}$$

where $\mathbf{K}_{k+1}$ is the Kalman Filter gain.

The model linearization of Equations (23) and (24) is obtained at each step using central finite differences. To estimate unknown parameters jointly with the states, the process

[4]Although variable, this feature is considered a parameter because it evolves significantly slower than the model's dynamics.

matrix is augmented with the directional derivatives of the unknown parameter. Since there is no prior knowledge on the parameter's evolution, a random walk model is used for the unknown parameter, i.e. $\dot{\mathbf{p}}(t) = \omega_p(t)$, being ω_p a zero-mean random variable. Thus, the augmented state-space model is described as follows

$$\begin{bmatrix} \dot{\mathbf{x}} \\ \dot{\mathbf{p}} \end{bmatrix} = \begin{bmatrix} \frac{\partial \mathbf{f}}{\partial \mathbf{x}} & \frac{\partial \mathbf{f}}{\partial \mathbf{p}} \\ \mathbf{0} & \mathbf{0} \end{bmatrix} \begin{bmatrix} \mathbf{x} \\ \mathbf{p} \end{bmatrix} + \begin{bmatrix} \omega \\ \omega_p \end{bmatrix} \tag{31}$$

B. GUIDE PROFILE VIRTUAL SENSOR: BOTTOM-UP PARAMETER ESTIMATION

To avoid interaction effects with other components, a model of the cabin and guiding system isolated from the other components is used. To isolate the component, the cable's tension is used as input and the remaining components are neglected. Consequently, this estimation model has 12 states corresponding to the cabin's translations and rotations. This model is represented in Figure 7, and further details are provided in Table 1.

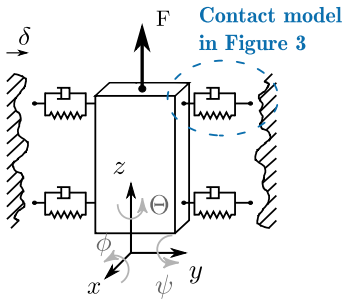

FIGURE 7. Representation of the cabin model and its degrees of freedom.

The parameter to be estimated is the deviation of the guiding rail with respect to the riding path, δ, defined in Equation (3). At each time step, this parameter is included in the linearized state-space model as described in Equation (31). The guide's alignment might be compromised in two directions: x and y, and since two guide rails are used, that would mean estimating four parameters as augmented states. To simplify the estimation, however, only one equivalent deviation is estimated, taking the following assumptions: (i) one of the guides is assumed to be perfectly aligned, and (ii) the guide's deviation is assumed to be only in x direction.

The contact parameters used in the model have a significant uncertainty, including the sliding shoe's clearance, the stiffness of the guiding rail and its supports or the contact damping. Estimating the exact value of these parameters would require extensive measuring campaigns with localized sensors at each sliding shoe. Instead, these parameters have been selected so that increments of the estimated parameter, δ, match the magnitude of a misalignment introduced in the test bench's guides in a controlled way. Therefore, although the estimated parameter is not exact representation of the guide's profile, it shows a good correlation with deviations of the guide with respect to the riding path.

TABLE 2. Parameters of the EKF for the estimation of the guide's deviation.

Model				Measurements	
State	**Q**	State	**Q**	Measurement	**R**
x [m]	10^{-2}	θ [rad]	10^{-4}	z_c [m]	10^{-4}
y [m]	10^{-2}	ϕ [rad]	10^{-4}	$\ddot{z}_c$ [m/s^2]	10^{-7}
z [m]	10^{-2}	ψ [rad]	10^{-4}		
$\dot{x}$ [m/s]	10^{-1}	$\dot{\theta}$ [rad/s]	10^{-3}		
$\dot{y}$ [m/s]	10^{-1}	$\dot{\phi}$ [rad/s]	10^{-3}		
$\dot{z}$ [m/s]	10^{-1}	$\dot{\psi}$ [rad/s]	10^{-3}		
δ[1] [m]	0.001				

[1] Augmented states

The parameters of the estimation are shown in Table 2, including the model's augmented states and measurements used. The filter tuning matrices are assumed diagonal matrices, i.e. the noise covariance **Q** and **R**. Table 2 shows the diagonal terms of these matrices associated with each state. The EKF is used to estimate jointly the states of the model and this equivalent guide alignment, δ. As observations of the estimation problem, the cabin position, z_c, and the cabin's vertical acceleration, $\ddot{z}_c$, are used. Although no dedicated observability assessment is performed, it should be noted that the number of sensors is too reduced to have a fully observable model. However, the unmeasured states (x, y, ϕ, θ, ψ and their derivatives) are bounded due to the guiding rails. Consequently, for these states it is fulfilled that $\lim_{t\to\infty} \|x(t)\| = 0$, making these states asymptotically stable, and the states of interest detectable [5], [41], i.e. z, $\dot{z}$, and δ. This detectability of the states of interest is confirmed by checking that their estimated covariances are asymptotically stable.

Although the system's natural frequencies are relatively low, a sampling frequency of $f_s = 1000$ Hz is used to ensure a good linearization of the nonlinear system. However, since the model only captures information up to circa 60 Hz (see Figure 6) all the measurements are low-passed filtered accordingly. Figure 8 shows the measurements required by this estimation: cable tension, F_c, cabin position, z, and cabin acceleration $\ddot{z}_c$.

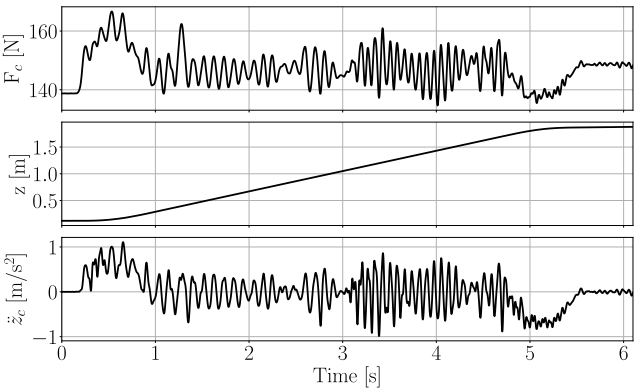

FIGURE 8. Measurements required by the estimation: cable tension, F_c, cabin position, z, and cabin acceleration $\ddot{z}_c$.

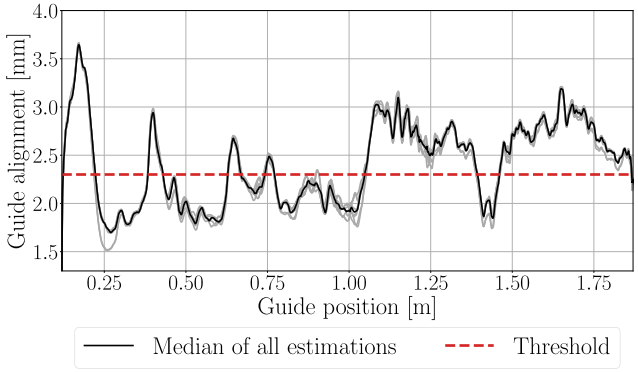

FIGURE 9. Estimated guiding rail's alignment (δ) and threshold (gray).

Figure 9 shows the result of the estimated guide alignment as a function of the guide's position. This figure shows the guide alignment estimated for 10 trips, and the median value of these trips. In addition, it shows the threshold selected for the estimated feature. The selection of this threshold is described later. It should be stressed, that often in the context of condition monitoring, the required parameter estimation accuracy is more relaxed than, for instance, the accuracy needed for a virtual sensor fed into a controller. This is because in condition monitoring often a parameter degradation rate is required rather than the actual parameter. In the current case, the estimated parameter should not be taken as an exact representation of the guide, but rather as an equivalent parameter showing localized deviations from the riding path. Thus, it gives an idea of the location and magnitude of the guide's misalignment. As explained earlier, the goal of this parameter is (i) to provide a feature related to the condition of the guide's installation, and (ii) to update the reference model so that it may predict the effect of changes on the guiding system. It should be stressed, that measuring the cable's tension likely requires dedicated sensors which are often unavailable. Therefore, this estimation process is a periodic inspection routine rather than a continuous monitoring process. Alternatives to continuously monitor the system using the presented models can be found in [3], [5].

C. GUIDE ALIGNMENT EVALUATION

Setting up a threshold for the estimated parameter requires a tradeoff between the ideal value of the parameter, in this case 0 mm, and the difficulty to reach that value. With a single estimation it is a challenging task to set a value to that threshold. A practical way to obtain a threshold, is to compare different installations and set the alignment threshold based on (i) the commonly obtained alignment, (ii) the required installation's quality, and (iii) economic limitations. To this end, the guide alignment estimated in 14 different configurations of the test bench's guiding system has been compared. This emulates a real scenario, where the parameter estimated in several installations is compared to set-up a threshold. It should be considered, that installations with different configurations, such as distance between guides, will likely require different thresholds.

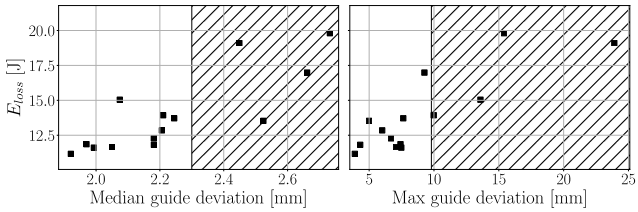

FIGURE 10. Estimated guide alignment for multiple configurations of the system against Energy loss.

Figure 10 shows the guide's deviation median and maximum values, and their corresponding energy losses. As a trade-off between the difficulty of having a proper guide alignment and an energy efficient installation, it was decided to set the threshold as the median guide alignment which covers the 70% of all installations, leading to a threshold of 2.3 mm. Setting the threshold based on the most common alignment ensures that it is not too restrictive, which would result in a high maintenance cost to adapt all the installations. The percentage of installations that should be covered by this threshold could be changed depending on the installation's demands, e.g. residential elevators will likely have less stringent efficiency demands than industrial elevators. Such selection follows often a heuristic approach based on economic indicators, which is out of the scope of this work. Thus, an arbitrary 70% has been selected.

The selected threshold is plotted in Figure 9, showing that the current guide alignment needs corrective actions at heights h = 0.1 m, 0.4 m, 1.1 to 1.3 m, and 1.5 to 1.8 m. In the following sections, the reference model updated with this misalignment is used to analyze the added value of correcting the alignment at these positions.

D. PRESCRIPTIVE ANALYTICS: WHAT-IF ANALYSIS

In addition to serve as a fault-sensitive feature, the guide alignment is used to update the updated reference model. Figure 11 compares the simulation of the reference model, and the measurements taken in the test bench for several variables: cabin and counterweight cable tensions F_c and F_{cw}, quadrature current i_q, cabin acceleration $\ddot{z}_c$, and cabin friction F^c_{fric}. Similarly, Table 3 provides error metrics to compare the simulated and measured variables.[5] Namely, the Root Mean Square Error (RMSE) and the Pearson Correlation Coefficient (ρ) are provided. While a good correlation is obtained in the magnitude of the simulated variables, a significant mismatch in vibration amplitude is present. This is because, although the estimated profile properly captures the dominant cause behind friction forces (i.e. the guide's alignment), several other non-updated elements affect the cabin's vibration. Namely, the controller's parameters, other guiding rail parameters, such as stiffness or damping, or noise in the model's input, i.e. ω_{ref}. Also, the vibrations induced by the guiding system, e.g. due to roughness or bumps in

[5]Friction is not measured, but indirectly obtained from the tension force and the cabin acceleration, and low-pass filtered.

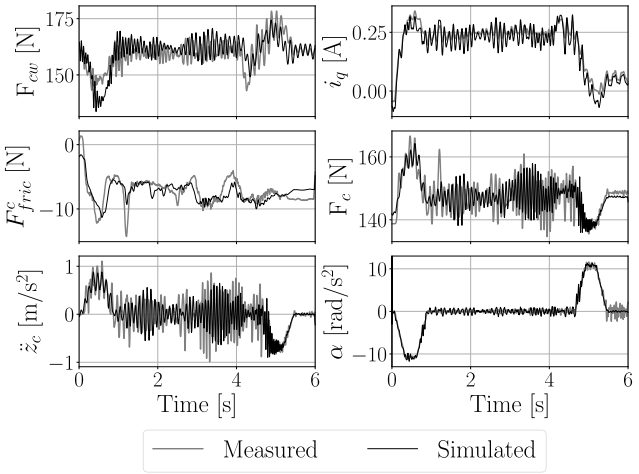

FIGURE 11. Comparison between the reference model simulation and the measured variables.

TABLE 3. Error metrics between simulated and measured variables.

Metric	F_{cw} [N]	i_q [A]	F^c_{fric} [N]	F_c [N]	$\ddot{z}_c$ [m/s^2]	α [rad/s^2]
RMSE	5.75	0.03	1.45	4.8	0.33	2.39
ρ	0.63	0.98	0.72	0.63	0.59	0.87

the guiding rails, are not properly captured by the model, and affect these variables. Therefore, this model should be limited to the study of the system's energy efficiency and shall not be used to assess the installation's comfort. To extend the model's capabilities, one should either (i) estimate the uncertain parameters through dedicated parameter estimation campaigns, or (ii) evaluate trends by statistically assessing the potential variations of each parameter, for instance, through Monte Carlo methods.

The threshold obtained in the previous sections gives a first quantitative evaluation of the guide's condition. However, it does not give information of the potential improvement upon corrective actions, or the suitability of carrying these actions out. This potential improvement will be evaluated using simulations of the updated reference model. In particular, three actions are studied through simulation: (i) correcting the most significant rail path deviations, (ii) improving the lubrication, assuming a 10% reduction in the friction coefficient, and (iii) both correcting the rail path and improving the lubrication. The guide alignment correction mentioned in points (i) and (iii) is simulated setting all the values of $\delta >$ threshold to 2.3 mm. The lubrication change mentioned in points (ii) and (iii) is assumed both for cabin and counterweight. The effect of lubrication on the friction coefficient of polymeric sliding shoes was studied in [42], showing a reduction of about 50% in the friction coefficient, with respect to dry friction. However, to keep a conservative assessment, the simulated reduction is limited to an arbitrary 10% reduction.

Table 4 shows the results of simulating these actions. Two different metrics are evaluated: (i) the total energy consumption of different components, and (ii) the overall efficiency. For point (i), the energy loss in the cabin's guide,

TABLE 4. Expected improvement in the system's energy efficiency based on the updated reference model simulation.

Metric		Original		Guide straightening		Lubrication	Both
		Meas.[1]	Sim.[2]	Meas.	Sim.	Sim.	Sim.
E_c	[J]	-12.46	-13.87	-10.63	-12.68	-12.43	-11.35
E_{cw}	[J]	-7.96	-7.71	-8.41	-7.71	-6.94	-6.94
E_{cb}	[J]	42.85	41.84	42.66	41.85	41.84	41.85
E_m	[J]	-21.42	-20.25	-22.78	21.44	22.46	23.53
η_t	[%]	52.35	48.42	55.37	51.28	53.70	56.30

[1] Measured; [2] Simulated

E_c, the energy loss in counterweight's guide, E_{cw}, the change in potential energy, E_{cb}, and the energy in the electric machine, E_m, are evaluated. Point (ii) is evaluated for the overall performance $\eta_t = E_{out}/E_{in}$, where E_{in} is the energy introduced in the system (either by the electric machine or by the positive change in potential energy) and E_{out} is the absorbed energy, e.g. by the machine in generator mode. Notice that in the case shown in the table, the input energy comes from the change in potential energy as the counterweight and cabin move, and the electric machine is in braking mode and thus "absorbing" energy. Furthermore, the gearbox friction losses are not considered, and are subtracted from the machine energy. It is also worth mentioning, that in relative terms, friction losses in this test bench are significantly larger than the losses expected in a real installation.

In addition to these simulations, the first corrective action, i.e. aligning the guiding rail, is done in the test bench, and its results are shown in Table 4. Lubrication correction has not been carried out because, currently, the test bench is not prepared to expel/redistribute the grease as it drops to the guide's bottom. Figure 12 shows the table's results in a visual way. As can be seen, the model has a good correlation with the test bench's efficiency, capturing well also the improvement on energy efficiency for the tested correction.

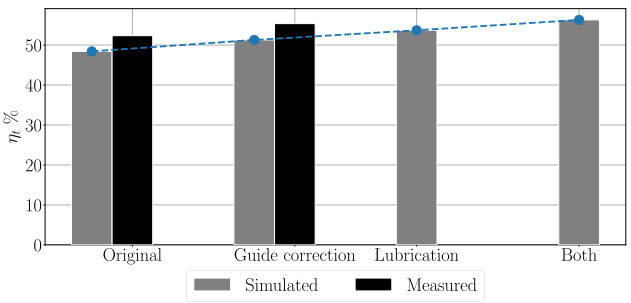

FIGURE 12. Comparison of different corrective actions.

These simulations show the potential effect of maintenance actions on the guiding system, aiding in the decision making. For instance, the simulation results suggest that just improving the lubrication may have a larger effect on the system's performance, on top of being probably a more cost effective solution.

After the corrective action, the guide's alignment has been estimated again to check its result. Figure 13 compares the original estimated alignment, with the threshold and with the current alignment. As can be seen, the corrective action had a

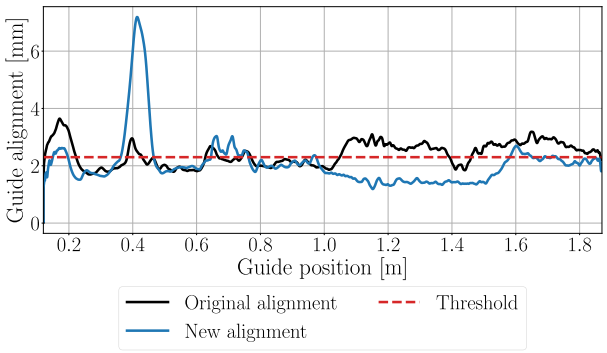

FIGURE 13. Guiding rail alignment before and after corrective actions.

good performance aligning the guide between h = 1.1 m and 1.8 m, and at h = 0.1 m. However, at height 0.4 m it resulted in an increased misalignment, because the alignment has probably deformed the whole guide, affecting areas which where not supposed to be changed. The requirement of further corrective actions could be evaluated again. However, as seen in Figure 12, the new alignment resulted in a better efficiency improvement than expected, and further corrective actions are not deemed necessary.

V. CONCLUSION

This study has presented a Digital Twin of a vertical transportation system, which is based on physics-based models and estimation algorithms. Emphasis was placed in developing its constitutive models in a scalable way, so that the Digital Twin may seamlessly adapt to different monitoring scenarios, such as high-fidelity simulation, virtual sensing, or bottom-up parameter estimation. In addition, this is of interest in industries where the product is highly customized and might thus require a customized model as well. In such models, it is essential to ensure that model reductions do not alter the physics of interest. To develop such system level models, acausal modeling tools have been identified as an attractive solution. In the presented case, such a Digital Twin has proven its effectiveness in the assessment of VTSs efficiency. Further work is required to extend this models to the assessment of the installation's comfort.

REFERENCES

[1] P. Hehenberger and D. Bradley, *Mechatronic Futures: Challenges and Solutions for Mechatronic Systems and Their Designers*. Cham, Switzerland: Springer, 2016.

[2] H. Van der Auweraer, S. Gillijns, S. Donders, J. Croes, F. Naets, and W. Desmet, "State estimation: A model-based approach to extend test data exploitation," in *Proc. 34th Conf. Expo. Struct. Dyn. Special Topics (IMAC)*, vol. 6. Cham, Switzerland: Springer, 2016, pp. 119–128.

[3] M. González, O. Salgado, J. Croes, B. Pluymers, and W. Desmet, "Application of state estimation to the monitoring of multiple components in nonlinear electro-mechanical systems," *Appl. Acoust.*, vol. 166, Sep. 2020, Art. no. 107371.

[4] U. Leturiondo, O. Salgado, L. Ciani, D. Galar, and M. Catelani, "Architecture for hybrid modelling and its application to diagnosis and prognosis with missing data," *Measurement*, vol. 108, pp. 152–162, Oct. 2017.

[5] M. González, O. Salgado, X. Hernandez, J. Croes, B. Pluymers, and W. Desmet, "Model-based condition monitoring of guiding rails in electro-mechanical systems," *Mech. Syst. Signal Process.*, vol. 120, pp. 630–641, Apr. 2019. [Online]. Available: https://linkinghub.elsevier.com/retrieve/pii/S0888327018307209

[6] E. Glaessgen and D. Stargel, "The digital twin paradigm for future NASA and U.S. air force vehicles," in *Proc. 53rd AIAA/ASME/ASCE/AHS/ASC Struct., Dyn. Mater. Conf., 20th AIAA/ASME/AHS Adapt. Struct. Conf. 14th AIAA*, Apr. 2012, pp. 1–14, doi: 10.2514/6.2012-1818.

[7] E. Negri, L. Fumagalli, and M. Macchi, "A review of the roles of digital twin in CPS-based production systems," *Procedia Manuf.*, vol. 11, pp. 939–948, 2017, doi: 10.1016/j.promfg.2017.07.198.

[8] H. Zipper, F. Auris, A. Strahilov, and M. Paul, "Keeping the digital twin up-to-date-process monitoring to identify changes in a plant," in *Proc. IEEE Int. Conf. Ind. Technol. (ICIT)*, Feb. 2018, pp. 1592–1597.

[9] R. Isermann and M. Münchhof, *Identification of Dynamic Systems: An Introduction With Applications*. Cham, Switzerland: Springer, 2010.

[10] D. Mayer, H. Atzrodt, S. Herold, and M. Thomaier, "An approach for the model based monitoring of piezoelectric actuators," *Comput. Struct.*, vol. 86, nos. 3–5, pp. 314–321, Feb. 2008.

[11] H. Dassanayake, C. Roberts, C. J. Goodman, and A. M. Tobias, "Use of parameter estimation for the detection and diagnosis of faults on electric train door systems," *Proc. Inst. Mech. Eng., O, J. Risk Rel.*, vol. 223, no. 4, pp. 271–278, Dec. 2009.

[12] S. Rahme and N. Meskin, "Adaptive sliding mode observer for sensor fault diagnosis of an industrial gas turbine," *Control Eng. Pract.*, vol. 38, pp. 57–74, May 2015, doi: 10.1016/j.conengprac.2015.01.006.

[13] C. D. Karlgaard and H. Shen, "Desensitised Kalman filtering," *IET Radar, Sonar Navigat.*, vol. 7, no. 1, pp. 2–9, Jan. 2013. [Online]. Available: http://digital-library.theiet.org/content/journals/10.1049/iet-rsn.2012%.0075

[14] G. Charles, R. Dixon, and R. Goodall, "Least squares method applied to rail vehicle contact condition monitoring," *IFAC Proc. Volumes*, vol. 41, no. 2, pp. 7451–7456, 2008, doi: 10.3182/20080706-5-KR-1001.01259.

[15] M. N. Chatzis, E. N. Chatzi, and A. W. Smyth, "On the observability and identifiability of nonlinear structural and mechanical systems," *Struct. Control Health Monitor.*, vol. 22, no. 3, pp. 574–593, Mar. 2015, doi: 10.1002/stc.456.

[16] B. Schleich, N. Anwer, L. Mathieu, and S. Wartzack, "Shaping the digital twin for design and production engineering," *CIRP Ann.*, vol. 66, no. 1, pp. 141–144, 2017, doi: 10.1016/j.cirp.2017.04.040.

[17] T. Mukherjee and T. DebRoy, "A digital twin for rapid qualification of 3D printed metallic components," *Appl. Mater. Today*, vol. 14, pp. 59–65, Mar. 2019, doi: 10.1016/j.apmt.2018.11.003.

[18] W. Luo, T. Hu, Y. Ye, C. Zhang, and Y. Wei, "A hybrid predictive maintenance approach for CNC machine tool driven by digital twin," *Robot. Comput.-Integr. Manuf.*, vol. 65, Oct. 2020, Art. no. 101974, doi: 10.1016/j.rcim.2020.101974.

[19] J. Leng, Q. Liu, S. Ye, J. Jing, Y. Wang, C. Zhang, D. Zhang, and X. Chen, "Digital twin-driven rapid reconfiguration of the automated manufacturing system via an open architecture model," *Robot. Comput.-Integr. Manuf.*, vol. 63, Jun. 2020, Art. no. 101895.

[20] L. Wright and S. Davidson, "How to tell the difference between a model and a digital twin," *Adv. Model. Simul. Eng. Sci.*, vol. 7, no. 1, Dec. 2020, Art. no. 13, doi: 10.1186/s40323-020-00147-4.

[21] F. Tao, H. Zhang, A. Liu, and A. Y. C. Nee, "Digital twin in industry: State-of-the-art," *IEEE Trans. Ind. Informat.*, vol. 15, no. 4, pp. 2405–2415, Apr. 2019.

[22] J. P. Andrew and S. Kaczmarczyk, *Systems Engineering of Elevators*. Mobile, AL, USA: Elevator World, 2011.

[23] O. Yaman, M. Baygin, and M. Karakose, "A new approach based on image processing for detection of wear of guide-rail surface in elevator systems," *Int. J. Appl. Math., Electron. Comput.*, vol. 4, pp. 296–300, Sep. 2016.

[24] J. M. Pagalday, X. Sagartzazu, A. Mardaras, and M. Calzada, "Implementation of a theoretical-experimental model for improving the comfort in lift installations," in *Proc. ISMA*, KU Leuven, 2004, pp. 3611–3624.

[25] P. Gołuch, J. Kuchmister, K. Ćmielewski, and H. Bryś, "Multi-sensors measuring system for geodetic monitoring of elevator guide rails," *Measurement*, vol. 130, pp. 18–31, Dec. 2018.

[26] I. Skog, I. Karagiannis, A. B. Bergsten, J. Harden, L. Gustafsson, and P. Handel, "A smart sensor node for the Internet-of-elevators-non-invasive condition and fault monitoring," *IEEE Sensors J.*, vol. 17, no. 16, pp. 5198–5208, Aug. 2017.

[27] A. Q. Flores, J. B. Carvalho, and A. J. M. Cardoso, "Mechanical fault detection in an elevator by remote monitoring," in *Proc. 18th Int. Conf. Electr. Mach.*, Sep. 2008, pp. 1–5.

[28] V. Venkatasubramanian, R. Rengaswamy, S. N. Kavuri, and K. Yin, "A review of process fault detection and diagnosis: Part III: Process history based methods," *Comput. Chem. Eng.*, vol. 27, no. 3, pp. 327–346, 2003.

[29] S. Boschert and R. Rosen, "Next generation digital twin," in *Proc. TMCE*, Las Palmas, Spain, 2018, pp. 209–217.
[30] Modelica Association. (2012). *Modelica—A Unified Object-Oriented Language for Systems Modeling-Language Specification-Version 3.3*. [Online]. Available: https://www.modelica.org/documents/ModelicaSpec33.pdf
[31] M. Otter, H. Elmqvist, and S. E. Mattsson, "The new modelica multibody library," in *Proc. 3rd Int. Modelica Conf.*, 2003, pp. 311–330.
[32] X. Arrasate, S. Kaczmarczyk, G. Almandoz, J. M. Abete, and I. Isasa, "The modelling, simulation and experimental testing of the dynamic responses of an elevator system," *Mech. Syst. Signal Process.*, vol. 42, nos. 1–2, pp. 258–282, Jan. 2014, doi: 10.1016/j.ymssp.2013.05.021.
[33] E. Esteban, O. Salgado, A. Iturrospe, and I. Isasa, "Model-based approach for elevator performance estimation," *Mech. Syst. Signal Process.*, vols. 68–69, pp. 125–137, Feb. 2016, doi: 10.1016/j.ymssp.2015.07.005.
[34] P. A. Fritzson, *Principles of Object-Oriented Modeling and Simulation With Modelica 2.1*. Hoboken, NJ, USA: Wiley, 2009. [Online]. Available: http://onlinelibrary.wiley.com/doi/10.1002/0470867906.ch2/summary
[35] P. C. Krause, O. Wasynczuk, S. D. Sudhoff, and S. Pekarek, *Analysis of Electric Machinery and Drive Systems*, vol. 75. Hoboken, NJ, USA: Wiley, 2013.
[36] ASME. (2006). *Guide for Verification and Validation in Computational Solid Mechanics*. pp. 1–15. [Online]. Available: http://scholar.google.com/scholar?hl=en&btnG=Search&q=intitle:Guide+for+Verification+and+Validation+in+Computational+Solid+Mechanics#1
[37] E. Esteban, O. Salgado, A. Iturrospe, and I. Isasa, "Design methodology of a reduced-scale test bench for fault detection and diagnosis," *Mechatronics*, vol. 47, pp. 14–23, Nov. 2017.
[38] F. Naets, J. Naets, and W. Desmet, "An online coupled state/input/parameter estimation approach for structural dynamics," *Comput. Methods Appl. Mech. Eng.*, vol. 283, pp. 1167–1188, 2015.
[39] N. Yokoyama, "Parameter estimation of aircraft dynamics via unscented smoother with expectation-maximization algorithm," *J. Guid., Control, Dyn.*, vol. 34, no. 2, pp. 426–436, Mar. 2011.
[40] D. Simon, *Optimal State Estimation: Kalman, H Infinity, and Nonlinear Approaches*. Hoboken, NJ, USA: Wiley, 2006.
[41] M. Boegli, "Real-time moving horizon estimation for advanced motion control: Application to friction state and parameter estimation," M.S. thesis, KU Leuven, Leuven, Belgium, 2014.
[42] X.-G. Zhang, H.-G. Li, and G. Meng, "Effect of friction on the slide guide in an elevator system," *J. Phys., Conf. Ser.*, vol. 96, Feb. 2008, Art. no. 012074.

MIKEL GONZÁLEZ was born in Barakaldo, Spain, in 1989. He received the master's degree in mechanical engineering from the University of the Basque Country, in 2012. He is currently pursuing the Ph.D. degree with KU Leuven, Belgium. After graduation, he has worked as a Stress Engineer for the aeronautic industry, making finite element and analytical calculations of CFRP and metallic aerostructures. Since 2015, he has been a Researcher with Ikerlan, Spain. His research interests include definition of virtual sensing solutions for condition monitoring of transportation systems.

OSCAR SALGADO was born in Vitoria-Gasteiz, Basque Country, in 1981. He received the degree in mechanical engineering, the M.Sc. degree (Hons.), and the Ph.D. degree in mechanical engineering from the University of the Basque Country, UPV-EHU, Spain, in 2004 and 2008. He joined the Mechanical Engineering Department, IKERLAN, in 2008, and moved to the Control and Monitoring Area, in 2016, where he is currently the Monitoring Team Leader. His research interests include kinematics and dynamics modeling of complex mechanical systems and manipulators, vibroacoustics, NVH, and modal analysis. Since 2014, he has been leading the Condition Monitoring Research conducted at IKERLAN, leading several industrial research projects and being author or coauthor of several papers and articles in this field.

JAN CROES received the Ph.D. degree in mechanical engineering from KU Leuven, in 2017. He is leading activities within the research group focusing on system level modeling of mechatronic systems with a particular focus towards energy efficiency, durability, and performance; and on the development of so-called virtual sensors, which are a key element in the exploitation of digital twins in model based testing.

BERT PLUYMERS received the Ph.D. degree from KU Leuven, in June 2006. From 2006 to 2008, he has worked as a Senior Researcher with the Noise and Vibration Research Group. In 2008, he is appointed by the KU Leuven Industrial Research Fund (IOF) as the Industrial Research Manager and the Senior Manager, in 2013, with a valorisation programme Dynamics 4.0. He is currently the contact and interface person for technology transfer for the Division Leuven Mecha(tro)nic System Dynamics (LMSD). In this role, he is bridging the gap between industry and academia. He is a Managerial Coordinator of a portfolio of national and international research projects. He is a member of the General Assembly of European Automotive Research Partners Association (EARPA)–as a Representative of KU Leuven and is a Secretary for the Foresight Group on Integrated and Connected Product Development–materials, manufacturing, and design tools. He is the representative for KU Leuven in the European Green Vehicles Initiative Association (EGVIA) A.i.s.b.l. and active in the working groups on Energy and Environment and Competitiveness as an Expert in ERTRAC, the European Road Transport Research Advisory Council. He is also a KU Leuven representative within the European Factories of the Future Research Association (EFFRA). In 2017, he is the General Chairman of the biennial ISMA-Noise and Vibration Engineering Conference in Leuven, Belgium. In 2014, he is a Business Developer with the Flemish Strategic Research Centre for the manufacturing industry–Flanders Make.

WIM DESMET received the Ph.D. degree in mechanical engineering from KU Leuven, Belgium, in 1998. He is currently a Full Professor in dynamics and mechatronics with the Department of Mechanical Engineering, KU Leuven, where he is also the Head of the Noise and Vibration Research Group, which currently counts more than 100 researchers. He has published more than 150 articles in international peer-reviewed journals and over 460 papers in international conference proceedings. He is a Promoter of 58 completed Ph.D. dissertations so far. He has been a Promoter of over 70 research projects, including several bilateral industrial research contracts, and multiple national and international research projects, including the co-ordination of European projects. His major research interests include vibro-acoustics, aero-acoustics, multibody dynamics, smart system dynamics, vehicle mechatronics, virtual prototyping techniques, noise control engineering, dynamics of lightweight materials, condition monitoring, uncertainty and variability in dynamics, green transportation, wind turbine dynamics, and mechatronic simulation.